

Thermo-mechanical and barrier properties of active sugar palm starch-chitosan biodegradable films containing *Moringa oleifera*

^{1,*}Hasan, M., ¹Rusman, R., ¹Khaldun, I., ¹Hanum, L., ¹Reza, S.N.D., ¹Nuzula, F.,
¹Zulfadli, Z. and ²Hasanah, U.

¹Department of Chemistry Education, Universitas Syiah Kuala, Darussalam Banda Aceh, 23311 Indonesia

²Department of Geophysical Engineering, Universitas Syiah Kuala, Darussalam Banda Aceh, 23311
Indonesia

Article history:

Received: 13 July 2023

Received in revised form: 12
September 2023

Accepted: 10 September 2024

Available Online: 9 August
2025

Keywords:

Biodegradable,
Active film,
Sugar palm starch,
Chitosan,
Moringa oleifera

DOI:

[https://doi.org/10.26656/fr.2017.9\(4\).230](https://doi.org/10.26656/fr.2017.9(4).230)

Abstract

Starch-chitosan blend films with added antioxidants derived from plant extract are promising materials for active food packaging. This study aimed to synthesize active food packaging films based on chitosan/sugar palm starch with the addition of *Moringa oleifera*. To achieve the desired goals, sugar palm starch (SPS)-chitosan (CH) films containing *Moringa oleifera* (MO) were developed, and the structure, physicochemical, barrier, antioxidant activity, and biodegradability performance of the films were characterized. X-ray Diffraction (XRD) analysis showed that no new scattering peaks appeared, indicating that the addition of MO did not alter the microstructure of the CH/SPS. All films exhibited ductile materials, where the addition of 1% MO increased tensile strength (TS) from 12.18 to 18.55 MPa while incorporating 3% MO increased elongation at break (EB) from 10.72 to 29.87%. The addition of MO increased the antioxidant activity from 17.47 to 48.65%. Atomic Force Microscopy (AFM) results indicated that the addition of 3% and 5% w/w MO produced a smoother film. It was concluded that CH/SPS-MO blend films exhibited excellent biodegradability, hence possess the potential for the intended application as an active film and can replace the use of pure CH/SPS film

1. Introduction

Research on the development of edible biodegradable food packaging films from natural polymeric materials has been increasing rapidly due to environmental pollution caused by plastic packaging made from non-biodegradable petrochemical raw materials (Arcana *et al.*, 2010). Biodegradable polymers are polymeric materials that may be degraded by enzymes and are typically made from a combination of cellulose, gelatin, starch, agar, gum, pectin and others (Chinaglia *et al.*, 2018; Nagar *et al.*, 2020). Several recent publications on biopolymers show the possible preparation of films through a combination of these compounds, ranging from fish gelatin crosslinked with alginate dialdehyde (Park *et al.*, 2021), gelatin-based functional films integrated with grapefruit seed extract and TiO₂ (Riahi *et al.*, 2021), quercetin-based chitosan-gelatin (Yadav *et al.*, 2020), and gelatin-based films integrated with tara gum (Nuvoli *et al.*, 2020).

Among a variety of biodegradable polymeric materials, starch and chitosan are very promising raw materials for the production of biodegradable films,

particularly for sustainable film packaging. Starch-based films offer advantages such as being inexpensive, non-toxic and simple to fabricate films (Ilyas *et al.*, 2019). Because starch has low mechanical properties, is hydrophilic, and is brittle, its application has been restricted (Jiang *et al.*, 2020). Meanwhile, chitosan, a biodegradable polymer with excellent mechanical properties, and the ability to form good films, is antimicrobial, and is abundant in nature and is a product of chitin deacetylation. The disadvantage is that chitosan has poor thermal characteristics and is rigid (Moeini *et al.*, 2020). Several recent studies on starch and chitosan-based biodegradable films have been published. The mechanical properties of blend films have been obtained from mixing chitosan with corn starch and yellow pumpkin starch (Hasan *et al.*, 2018; Frick Pavoni *et al.*, 2019). The active film of corn starch coated with a chitosan oligomer serves as an antimicrobial agent (Castillo *et al.*, 2017). The thermal properties of chitosan-based films can be improved by blending them with brown rice starch (Hasan, Gopakumar, Olaiya *et al.*, 2020).

Considering that food spoilage is mainly influenced

*Corresponding author.

Email: muhammadhasan.kimia@usk.ac.id

by oxidation and microbial degradation, food film packaging must be not only elastic and strong but also have suitable antimicrobial and antioxidant properties (Mozafari *et al.*, 2006). As a result, naturally active substances such as essential oils could be used to create active films for food packaging based on starch-chitosan composites. Ma *et al.* (2022) have synthesized flexible antimicrobial films with chitosan nanoparticles and potato peel polyphenols. Istiqomah *et al.* (2022) also reported that the physical, mechanical, and antibacterial properties of chitosan films modified with *Discorea alata* starch have been improved. The antibacterial activity of starch film combined with chitosan nanocapsules loaded with cinnamon oil against *Escherichia coli* or *Bacillus* was exhibited, and the freshness of strawberries could be prolonged (Ferreira *et al.*, 2020). The presence of polyphenolic compounds promotes the antioxidant activities of the film through the chelation mechanism, preventing lipoxygenase enzyme activity and scavenging free radicals (Talón *et al.*, 2017). Several papers have been published on the use of natural active compounds to improve the antibacterial and antioxidant characteristics of starch-chitosan composite films, including lemongrass, garlic and aloe vera (Istiqomah *et al.*, 2022), cinnamon and clove essential oil (Choo *et al.*, 2021), rosemary and ginger (Lauriano Souza *et al.*, 2019), and extra virgin olive oil (Hasan, Rusman, Khaldun *et al.*, 2020).

Another naturally active compound that has the potential to be used as an antioxidant is *Moringa oleifera* L. It shows strong antioxidant activity due to its high content of flavonoids and phenolic compounds, especially in its leaves (Brilhante *et al.*, 2017). *Moringa oleifera* (MO), a tropical plant from the *Moringaceae* family, mainly grows in Asia and Africa (Abubakar and Benjamin, 2019). Because of its bioactive compounds, such as phenolic acids, flavonoids, isothiocyanates, tannins, and saponins, which are present in significant amounts, MO has properties in the health sector for the treatment of high cholesterol, high blood pressure, diabetes, insulin resistance, non-alcoholic liver disease, cancer and infection in general (Vergara-Jimenez *et al.*, 2017). Although the antioxidant activity of MO extract is very high, there are still very few publications on the incorporation of MO into biopolymer matrix-based food packaging. Rodríguez *et al.* (2020) developed an antioxidant edible film made from papaya, which incorporated *M. oleifera* and ascorbic acid. Ryandari and Multazam (2023) reported that the addition of MO leaf extract enhances the antioxidant activity of chitosan-alginate film, showcasing increased radical scavenging activity with higher extract concentrations. A Khorasan wheat starch film containing moringa leaf extract has good antioxidant activity and a good ultraviolet light-

blocking ability (Ju *et al.*, 2019). However, no studies have been published regarding the incorporation of MO into starch and chitosan-based film biopolymers. This paper reports an in-depth study on the addition of MO leaf extract and its effect on the structure, thermal and mechanical properties, physico-chemical properties, and antioxidant activities of CH/SPS-MO composite films. To the best of our knowledge, this is the most recent publication on active films prepared from sugar palm starch-chitosan with the addition of MO extract. Structure, barrier characteristics, thermal properties, tensile strength, antioxidant activities, and biodegradability were already characterized in the active films that were produced. The findings of this study provide a new formulation for manufacturing active films from sugar palm starch-chitosan that can be used as a substitute for commercial packaging films made from petrochemical raw materials.

2. Materials and methods

2.1 Materials

SPS powder (37% amylose, 63% amylopectin) was purchased from Sago Aren Co., Ltd., Indonesia (Sea Horse brand). *Moringa oleifera* Lam. leaf was purchased from a local market (Banda Aceh, Indonesia), chitosan powder (particle size 200-300 mesh; molecular weight 102 KDa; 96.24% degree of deacetylation) was purchased from Chimultiguna Co., Ltd. (Indramayu, Indonesia), glacial acetic acid, 2,2-diphenyl-1-picrylhydrazyl, and glycerol were purchased from Sigma Aldrich (Darmstadt, Germany).

2.2 Preparation of *Moringa oleifera* Lam. leaf extract

Moringa leaf extract powder was prepared using the maceration method developed by Lee *et al.* (2016) with a slight modification. Approximately 50 g of Moringa leaf powder was soaked for 48 hrs in 100 mL of 70% ethanol solvent while being continuously stirred. Then, the solvent in the filtrate was removed using a rotary vacuum evaporator and subsequently dried.

2.3 Preparation of films

Film-forming solutions (3% w/v) with different MO contents (1%, 3% and 5%) of total weight were prepared to produce four different blends for the films, following the previous procedure (Hasan, Gopakumar, Olaiya *et al.* 2020). SPS and CH solutions were prepared according to the procedures of Ilyas *et al.* (2019) and Jumaidin *et al.* (2016). These SPS and CH solutions, MO (0, 1, 3 and 5% w/w), and glycerol (30% w/w) were mixed while being stirred and kept at a temperature of 90°C. After 3 hrs, all solutions were cooled to room temperature and poured into acrylic casting plates (10 cm × 10 cm).

Before further analysis, the films were stored at 25°C and 55±2% relative humidity (RH) for 36 hrs.

2.3 Fourier transform infrared spectroscopy

To determine the effects of the addition of MO on the vibration pattern of the functional groups in CH/SPS-MOs were determined by using Fourier transform infrared spectroscopy (FTIR) (Shimadzu IR Tracer-100 FTIR Spectrometer, Japan). Spectra with a resolution of 4 cm⁻¹ were recorded in the wavenumbers ranging from 600 to 4000 cm⁻¹ (Hasan, Chong, Jafarzadeh *et al.*, 2019). The impact of MO on vibration patterns of functional groups in CH/SPS-MOs was examined through FTIR analysis using a Shimadzu IR Tracer-100 FTIR Spectrometer from Japan.

2.4 Thickness and water uptake

The film thickness was measured at three random locations using a digital micrometer (Mitutoyo IP 65, Japan). Water uptake from the sample films was determined gravimetrically using the method developed by Siti Waqina *et al.* (2016). The percentage of water uptake from the film sample was calculated using Equation (1).

$$\text{water uptake} = \frac{W_f - W_i}{W_i} \times 100\% \quad (1)$$

where W_i and W_f are the initial and final weights, respectively. Theoretically, the adsorption process can be explained using Fick's second law of diffusion (Equation 2) (Pelissari *et al.*, 2017). The initial kinetics of sorption can be stated as follows:

$$\frac{M_t}{M_\infty} = \frac{4}{L} \sqrt{\frac{Dxt}{\pi}} \quad (2)$$

where M_t is the mass of water (g) absorbed over time t , M_∞ is the mass of water (g) absorbed at thermodynamic equilibrium, and L is the film thickness. The diffusion coefficient, D , can be determined as the slope of a line fitted to the straight-line portion of R^2 over 99%, where the line is plotted using M_t/M_∞ versus \sqrt{t} .

2.5 Water vapor permeability

The water vapor permeability (WVP) values of the films were determined according to the procedure reported by Khalil *et al.* (2019) with slight modifications. The film was cut into a circular form and then positioned to cover the test cup, which had been filled with distilled water. The test cup was placed in a desiccator containing silica gel as a desiccant at 50±5% RH and 25±2°C. For 6 hrs, the test cup was weighed every hour. The difference in test cup weight was then plotted, the slope of the curve was calculated with a regression coefficient >0.99, and the WVP value was determined using Equation (3).

$$VWP (.Pa^{-1}s^{-1}m^{-1}) = \frac{\Delta w \times L}{t \times A \times \Delta P} \quad (3)$$

where W is the change in test weight of cup (g), t is time (h) and A is the area of the film surface (m²), L is the thickness of the film and ΔP is a pressure difference between the desiccators and the test cup ($\Delta P = 3169$ Pa) (Karimi Sani *et al.*, 2019).

2.6 X-ray diffraction

X-ray diffraction (XRD) data were obtained from measurements performed by the Shimadzu XRD-7000 Maxima-X. (Japan). The measurement procedures were derived from the method described by Hasan, Gopakumar, Olaiya *et al.* (2020).

2.7 Atomic force microscopy

The morphology and surface roughness of the films were examined through topographic analysis using multi-mode atomic force microscopy (AFM) with a type E piezoelectric scanner (Veeco Instruments, USA). Three-dimensional images of the film surface (20 μm × 20 μm) and surface roughness parameters of R_a and R_q were determined. Films with dimensions of 1.5 cm × 1.5 cm were used for the analysis with a force constant of 42 N m⁻¹ and a resonant frequency of 320 kHz. The raw image was processed using image analysis and multi-mode presentation software.

2.8 Mechanical properties

The tensile strength and elongation of the films were tested using an ASTM D638 Plastics Tension 1144 instrument (MTS EM) from the USA. Samples with a size of 4.0 cm × 1.0 cm were prepared and tested using a load of 5 kN and a speed of 0.030 m/min (Hasan, Chong, Jafarzadeh *et al.*, 2019). Before testing, the specimens were stored at room temperature for 24 hrs with a relative humidity of 52%.

2.9 Thermal properties

The thermal behavior of the films was analyzed using a DTG-60 thermogravimetric analyzer (Shimadzu, Japan). Before the analysis, the films were stored at 25°C with a relative humidity of 52%. Small film pieces weighing 5.0 mg were tested by heating them from 30°C to 600°C at a heating rate of 15°C/min under an N₂ atmosphere with a feed rate of 20 mL/min (Suriyatem *et al.*, 2018).

2.10 Antioxidant activity test

The antioxidant activity of the films was measured by assessing their ability to capture 2,2-diphenyl-1-picrylhydrazyl (DPPH) radicals, following the method described by Caetano *et al.* (2017). In this method, 1.97

mg of DPPH was dissolved in 50 mL of ethanol to obtain 0.1 mM DPPH solution, which was stored in a dark bottle. Next, 50 mg of each film sample was dissolved in 10 mL of 96% ethanol and stirred with a magnetic stirrer for 1 min. The solution was left for 2 hrs, then centrifuged for 10 mins. Subsequently, 1.0 mL of each film solution was mixed with 4.0 mL of 0.1 mM DPPH, and the mixture was incubated for approximately 30 min in the dark. The absorbance was measured at a wavelength of 517 nm using a UV-Vis spectrophotometer, and the percentage of DPPH radical scavenger activity was determined using (Equation 4).

$$\text{DPPH Scavenging Activity (\%)} = \frac{\text{Abs}_{\text{DPPH}} - \text{Abs}_{\text{Film}}}{\text{Abs}_{\text{DPPH}}} \times 100 \quad (4)$$

Where Abs_{DPPH} is the absorbance of the DPPH solution, and Abs_{Film} is the absorbance of the film sample.

2.11 Biodegradation test

A biodegradation test was conducted based on the method described by Zain *et al.* (2018) with slight modifications. Films were prepared with dimensions of 2.5×2.5 cm, and their initial weight was recorded. A plastic container was filled with compost media with a 20 cm thickness, and the film was embedded in the media up to a depth of 10 cm. The films were then removed from the media after 5, 10, 15, 20 and 25 days, immersed in 70% ethanol, and dried in an oven at 50°C for 24 hrs.

2.12 Statistical analysis

The study used SPSS software to analyze the data, which was assessed for each sample at least three times and presented as the mean \pm standard deviation (SD). ANOVA with a significance level of $p < 0.05$ was used to evaluate the data, and Duncan's multiple ranges at $p < 0.05$ were used to determine significant differences between groups.

3. Results and discussion

3.1 Fourier transform infrared spectroscopy analysis

FTIR spectra were used to analyze patterns of molecular interactions through functional groups of sugar palm starch-chitosan and MO blend films. Figure 1 presents the FTIR spectra of the biocomposite films from CH, SPS, and CHSPS-MOs. Based on the spectra, it seems that MO, CH, SPS, and the CH/SPS-MO blended film showed absorption peaks in the region of almost the same wavenumber. Peaks at $3700\text{--}3000$ cm^{-1} are assigned to the stretching vibration of the free hydroxyl group (O-H) in MO, CH, SPS, and the CH/SPS (Ju *et al.*, 2019; Hasan *et al.*, 2022). Meanwhile, the peak at 2924

cm^{-1} is attributed to the stretching vibration of C-H (Rodríguez *et al.*, 2020). The absorption peak pattern of the CH/SPS matrix was not significantly altered by the addition of MO. Only the amplitude of absorption peaks of certain functional groups was observed to have changed. All samples displayed characteristic peaks at wavenumbers 1021, 1405, 1551, and 1642 cm^{-1} , which correspond to the stretching vibrations of C-O-C, C-N, N-H bending, and C=O, respectively (Lee *et al.*, 2016). The addition of MO increased the amplitude of the O-H stretching vibration peak within the $3000\text{--}3300$ cm^{-1} region, indicating enrichment of the O-H group from the MO compound. This increase in the film's absorption capacity was consistent with previous findings in edible films incorporating *Moringa oleifera* (Rodríguez *et al.*, 2020). Hydrogen bonding between the starch-chitosan matrix and compounds within the MO extract caused a shift in the wavelength of several functional groups. Yadav *et al.* (2020) reported similar results.

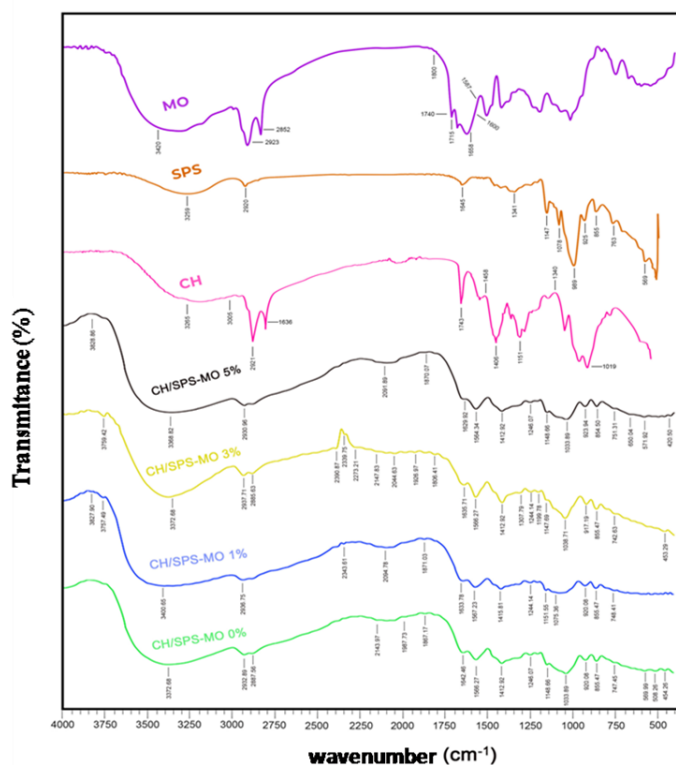


Figure 1. FTIR spectra of MO, CH, SPS, and CHSPS-MOs film samples.

3.2 Thickness and water uptake

Thickness and water uptake data from CH, SPS, and CH/SPS-MOs films are presented in Table 1. The thickness of the film was significantly ($p < 0.05$) influenced by the addition of 3% and 5% w/w MO extracts. The highest thickness value of the film was associated with the addition of 3% w/w MO extract, while the lowest value was attributed to the film without the addition of MO extract. This was most presumably associated with the presence of more hydroxyl groups from MO, which increased the interfacial space between

Table 1. Film thickness, kinetic parameter (M_{∞} , diffusion coefficient, D), and WVP of CH/SPS and all CH/SPS-MO blend films.

	Thickness (mm)	M_{∞} (%)	D ($10^{-4}\text{mm}^2\text{s}^{-1}$)	WVP ($10^{-10}\text{g}\cdot\text{Pa}^{-1}\text{s}^{-1}\text{m}^{-1}$)
CH	0.22±0.01 ^c	42.24±3.25 ^b	1.64±1.12 ^a	1.52±0.08 ^{bc}
SPS	0.14±0.00 ^a	61.05±2.53 ^c	2.75±0.44 ^{ab}	1.74±1.02 ^c
CH/SPS-MO 0%	0.13±0.01 ^a	17.15±7.13 ^a	1.57±0.28 ^a	0.70±1.59 ^a
CH/SPS-MO 1%	0.14±0.01 ^a	53.17±8.47 ^b	2.62±0.44 ^{ab}	1.29±0.18 ^b
CH/SPS-MO 3%	0.21±0.01 ^c	49.37±4.19 ^b	3.84±1.35 ^b	2.19±0.09 ^d
CH/SPS-MO 5%	0.17±0.00 ^b	64.07±0.89 ^c	3.79±0.26 ^b	1.91±0.04 ^c

Values are presented as mean±SD. Values with different superscripts in the same column are statistically significantly different ($p<0.05$).

molecular chains (Frick Pavoni *et al.*, 2019). In a previous study, the existence of hydrophilic and hydrophobic groups in the polymer matrix was reported to contribute to the existence of sponge-like structures (Hasan, Rusman, Khaldun *et al.*, 2020). Water absorption is an essential aspect to consider when selecting a packing film. Figure 2 depicts the water uptake capacity trend of CH, SPS, and all CH/SPS composite films with varying MO concentrations. All films showed very fast absorption of water, where within 20 s all film samples have reached optimum absorption. This is probably influenced by the presence of free hydroxyl groups in the film matrix, which form hydrogen bonds with water (Surya *et al.*, 2020). The water absorption ability of a film is associated with differences in the chemical potentials of water molecules bound in a composite film matrix (Sousa *et al.*, 2019). The CH/SPS-MO 0% film has a lower water absorption capacity than other films, at 17.15% absorption. The addition of MO extract increased the adsorption capacity significantly ($p<0.05$) from the film. This is probably due to the enrichment of the hydroxyl groups in the film matrix due to the addition of the MO extract. This result corroborates the results of the FTIR analysis. However, the films obtained through this study have relatively lower adsorption capacities for water. This is due to strong intermolecular interactions between starch,

chitosan, and MO extracts, which prevent water molecules from permeating the film. Table 1 indicates a significant difference ($p<0.05$) in the diffusion coefficient (D) between samples without MO extract and those with varying concentrations of MO extract added. The addition of MO extract to the CH/SPS matrix resulted in a significant increase in the D value. The presence of hydrophilic groups within the polymer matrix promotes the formation of a sponge-like structure, creating free volume in the molecular microstructure, which facilitates water molecule penetration into the film (Bilbao-Sainz *et al.*, 2011). These findings are consistent with those reported by Fonseca-García *et al.* (2021).

3.3 Water vapor permeability

The WVP values of the films were presented in Table 1. The results showed that the films with MO extract had higher WVP values than the SPS/CH film without MO extract. This was due to the increase in the number of hydroxyl groups in the film matrix that interacted with water molecules as a result of incorporating MO extract. In contrast, the SPS/CH film without MO extract had a lower WVP value because of the hydrogen bonds created between the NH_2 group in chitosan and the OH group of starch, which reduced the interaction with water molecules (Luchese *et al.*, 2018). The study's findings were consistent with a previous study that demonstrated how the addition of 2% and 5% w/w EVOO increased the WVP value of the CH/SPS-EVOO film (Hasan, Rusman, Khaldun *et al.*, 2020). However, the WVP value in this study was lower than the WVP values reported by Ribeiro Sanches *et al.* (2021) for blended films of starch, red cabbage, and sweet whey, which ranged from 1.2×10^{-7} to 5.4×10^{-7} $\text{g}\cdot\text{m}^{-1}\text{h}^{-1}\text{Pa}^{-1}$.

3.4 X-ray diffraction

The X-ray diffraction (XRD) pattern shown in Figure 3 illustrates the CH, SPS, and CH/SPS films containing MO extract. The scattering peak of the SPS film is observed at 2Θ of 15° , 16.5° , and 23° , which correspond to A-type crystals from starch. On the other hand, the CH film exhibits a diffraction peak at 2Θ

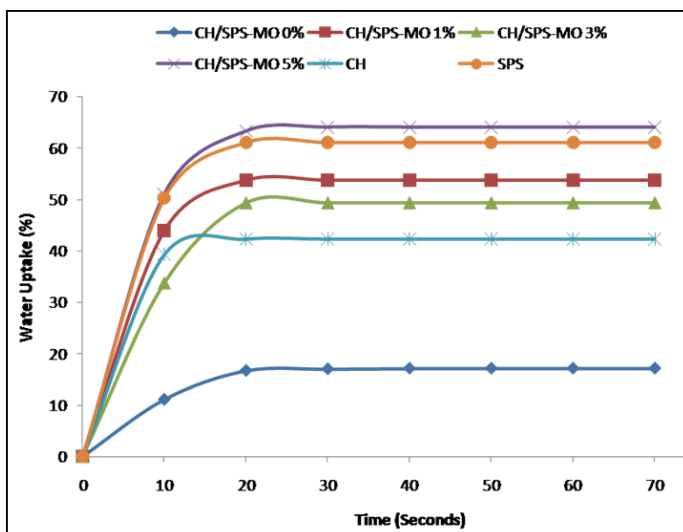


Figure 2. Water uptake performance of CH, SPS, and all CH/SPS-MOs film samples.

around 20° and 27°, indicating the most amorphous structure (Suriyatem *et al.*, 2018). The broad peak observed in the XRD pattern indicates the presence of an amorphous region, while the sharp peak represents a crystalline region, revealing that the film samples have a semi-crystalline structure. The addition of MO extract to the blend of SPS and CH films leads to a decrease in the intensity of the crystalline structure of SPS. This is attributed to the occurrence of microstructural interactions during the formation of the biocomposite (Fang *et al.*, 2019). The X-ray diffraction (XRD) analysis showed that there were no new scattering peaks present in the CH/SPS blend after the addition of MO extract. This suggests that the microstructure of the blend was not affected by the presence of MO. This finding is consistent with previous research conducted by Hasan, Gopakumar, Olaiya *et al.* (2020). The peaks observed at 21.3° and 19.8° were attributed to the Vh structures in chitosan-coated phosphorylated starch films (Merino *et al.* 2018).

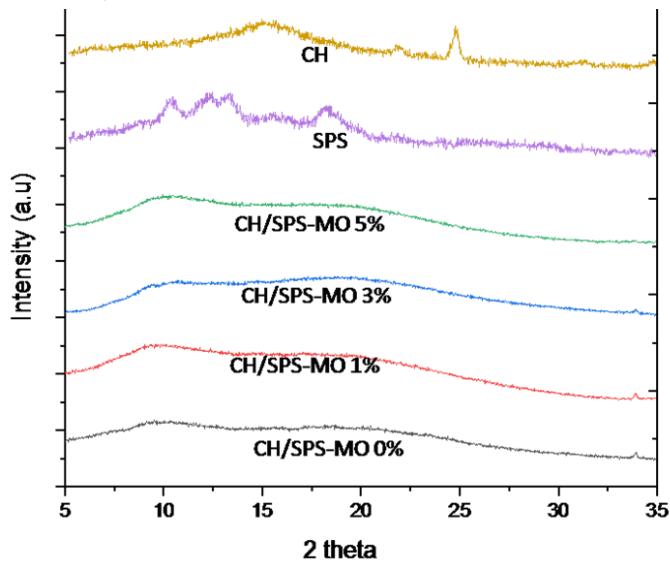


Figure 3. XRD pattern of CH, SPS, and CH/SPS-MOs films.

3.5 Atomic force microscopy

AFM was used to characterize the surface roughness of CH, SPS, and all CH/SPS-MOs films, both qualitatively and quantitatively. Figure 4 demonstrates AFM images along with surface roughness parameters, Ra and Rq, of CH, SPS, and CH/SPS-MOs films, and it is observed that all films exhibited a smooth surface, except for neat CH, SPS, and CH/SPS-MO 1% samples, which are slightly rough. No residual CH or SPS appeared in the blend films, demonstrating that the blend of SPS and CH was quite compatible (Dai *et al.*, 2019). This shows that the addition of 3% and 5% w/w MO were homogeneously distributed to the film matrix. This observation was in agreement with the results reported by Ilyas *et al.* (2019).

The CH film had higher Ra and Rq values than the

other samples, which were 82 nm and 100 nm, respectively, while the lowest Ra and Rq values were 18 nm and 22 nm, respectively, which was attributed to the film with no addition of MO. The smooth surface of the film was due to the formation of relatively stronger hydrogen bonds between CH, SPS, and MO upon film formation (Chollakup *et al.*, 2020). However, the Ra value of the results of this study was lower than the results reported by Tessaro *et al.* (2021), where the gelatin-chitosan-based film containing pitanga leaf hydroethanolic extract films had Ra values within 74.7-87.5 nm.

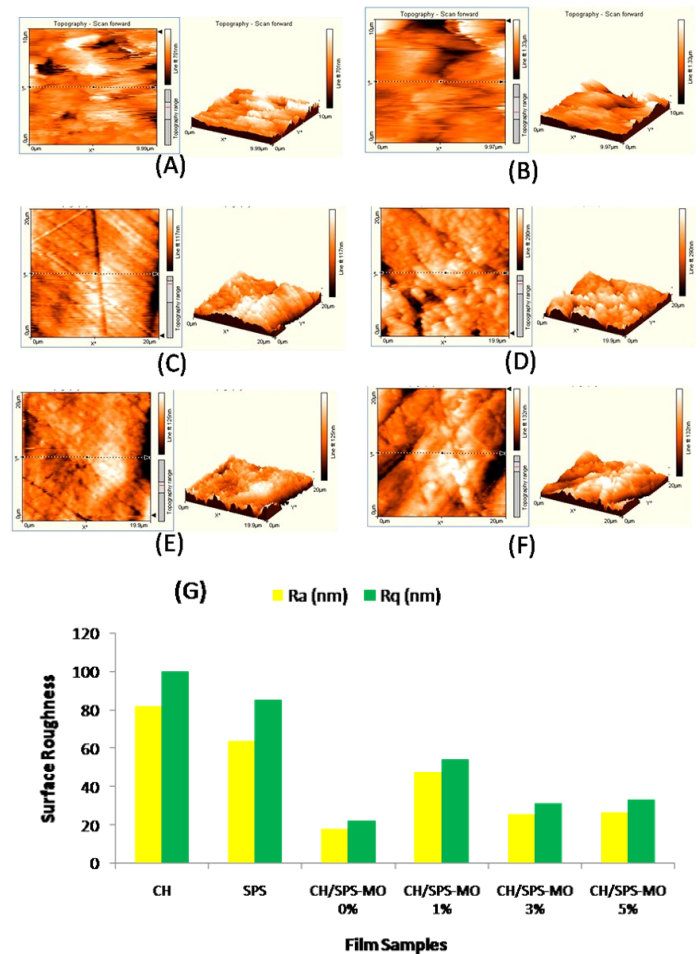


Figure 4. AFM images of: (A) CH; (B) SPS; (C) CH/SPS-MO 0%; (D) CH/SPS-MO 1%; (E) CH/SPS-MO 3%; (F) CH/SPS-MO 5%; (G) surface roughness curve of films.

3.6 Mechanical properties

The deformation behavior of a film can best be evaluated via a stress-strain curve. Figure 5 displays stress-strain curves from the CH, SPS, and CH/SPS-MO 0%, CH/SPS-MO 1%, CH/SPS-MO 3%, and CH/SPS-MO 5% blend films. Meanwhile, Table 2 summarizes the TS and EB values of CH, SPS, and all samples of CH/SPS-MOs films. It has been shown that all films constitute ductile materials, with the curve displaying two major sections, namely elastic and plastic deformation.

Table 2. Mechanical properties and antioxidant activity of CH, SPS, and CH/SPS-MOs blend films.

Film Samples	TS (MPa)	EB (%)	Antioxidant activity (%)
CH	7.92±1.93 ^a	7.74±3.53 ^b	34.56±1.74 ^a
SPS	7.64±2.34 ^a	3.77±3.59 ^a	46.05± 1.30 ^b
CH/SPS-MO 0%	12.18±4.36 ^b	10.72±5.52 ^b	20.80±16.04 ^a
CH/SPS-MO 1%	18.55±6.13 ^c	13.86±6.91 ^b	35.86±20.11 ^a
CH/SPS-MO-3%	15.40±4.03 ^b	29.87±1.38 ^c	40.60±6.26 ^b
CH/SPS-MO 5%	8.74±3.75 ^a	19.44±13.28 ^b	48.65±3.69 ^b

Values are presented as mean±SD. Values with different superscripts in the same column are statistically significantly different ($p < 0.05$).

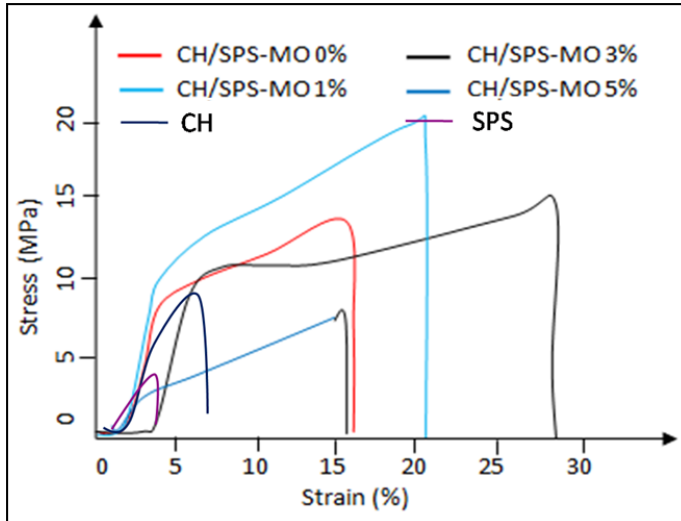


Figure 5. Stress-strain curve of CH, SPS, and CH/SPS-MOs composite films.

The TS and EB values of neat chitosan (CH) and sugar palm starch (SPS) were lower than those of all CH/SPS-MOs composite samples. The blending of chitosan with sugar palm starch and the incorporation of MO extract significantly ($p < 0.05$) increased the TS and EB values of the CH/SPS film. The highest TS values were shown by CH/SPS-MO 1% with the value of 18.552 MPa, while the lowest TS value was 8.738 MPa assigned to CH/SPS-MO 5%. Meanwhile, the highest EB value was associated with CH/SPS-MO 3% with a value of 24.872% and the lowest one was 10.717% attributed to the CH/SPS-MO 0% sample. The increase in TS and EB values of the CH/SPS film was due to more molecular

interactions between MO extracts and the film matrix. The distribution and density of intra- and intermolecular interactions between polymer molecular chains in the film matrix are responsible for mechanical properties (Kanatt, 2020). Similar results were reported by Rodríguez *et al.* (2020) that the edible film from papaya, which incorporated MO, has a higher TS value than the control film, and the value is in the range 0.1–1.1 MPa. The addition of 5% MO reduces the mechanical properties, which is due to a decrease in the cohesion force of the film, which was triggered by obstruction of intermolecular interactions of the polymer chain (Ju *et al.*, 2019). Ju *et al.* (2019) reported a similar result, showing that the addition of MO extract decreased the TS value of Khorasan wheat starch.

3.7 Thermogravimetric analysis

Thermogravimetric analysis (TGA) is a thermal analysis technique that can be used to evaluate the thermal stability of a material, and we use it to assess composite films for sustainable food packaging. Figure 6 displays TGA curves and their derivative (DTG) of CH, SPS, and all CH/SPS-MOs blend films. Table 3 shows the thermal characteristic parameters Tonset (initial decomposition temperature) and Tmax (maximum decomposition temperature).

3.8 Antioxidant activity

Antioxidant activity data of all samples are tabulated

Table 3. TGA profile of CH, SPS, and CH/SPS-MOs blend films.

Film samples	Thermal degradation temperature (°C)					Residue (%)
	T _{onset} ^a	T _{max}	T ₂₀ ^c	T ₅₀ ^c	T ₇₀ ^c	
CH	216.60	491.80	238.10	396.20	549.60	19.59
SPS	271.20	421.80	282.00	302.10	313.90	0.00
CH/SPS-MO 0%	244.55	370.90	200.37	317.71	353.68	10.60
CH/SPS-MO 1%	239.84	365.44	170.29	321.26	417.38	23.40
CH/SPS-MO 3%	234.93	376.78	191.23	325.94	491.67	27.20
CH/SPS-MO 5%	238.96	371.01	214.79	328.73	600.00	30.00

^a Temperature which initial degradation

^b Temperature maximum of degradation

^c Degradation temperature with 20%, 50%, and 70% of weight loss

^d Residue at the temperature of 600°C.

in Table 2. The results showed that the antioxidant activity of CH/SPS films increased significantly ($p < 0.05$) with the addition of different amounts of MO extract, up to 5.0% (w/w). The antioxidant activity of the films obtained in this study was in the range of 20.80-48.65%. The lowest antioxidant activity (20.80%) was associated with CH/SPS-MO0%, denoting films without the presence of MO extract, whereas the highest antioxidant activity (48.65%) was observed in films containing 5.0% (w/w) of MO. Similar results were reported by Zeng *et al.* (2021), where chitosan film that incorporated pomegranate peel had an antioxidant activity that ranged from 13.91-52.05%. The results may be influenced by the phenolic compounds in MO extract, which act as a free radical scavenger (Calabria *et al.*, 2020).

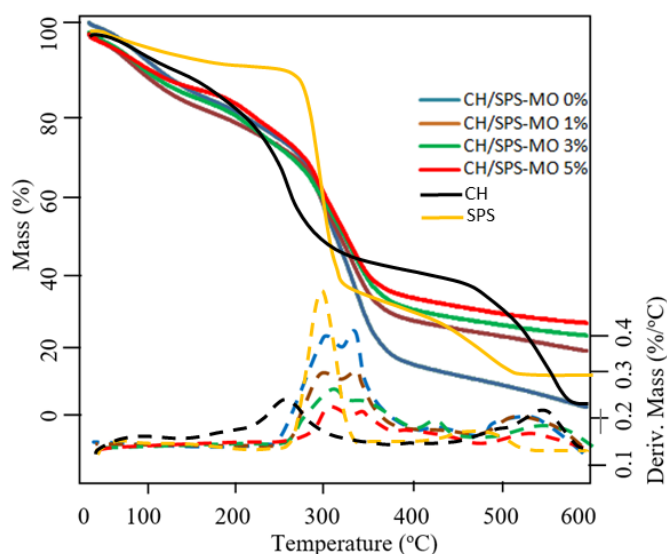


Figure 6. TGA and DTG curves of CH, SPS, and CH/SPS-MOs films.

3.9 Biodegradation properties

Soil burial of a material can be used as an indicator for the biodegradation process by moisture and microorganisms during the burial period. The biodegradation test results of CH, SPS, and all CH/SPS-MOs films samples are shown in Figure 7. Figure 7(A) depicts the outer structure of each sample tested for biodegradability at varied burial times. After 5 days of burial, there was a change in color and physical harm to the sample, indicating that the film had been attacked by microbes. After 10 days, rapid degradation, marked by cracking into small pieces, was observed. The neat sugar palm starch film was biodegradable after 20 days of burial. This finding was strongly in accordance with previous results, where the biodegradation mechanism of the brown rice starch/chitosan film began to crack and crumble after 10 days of burial (Hasan, Gopakumar, Olaiya *et al.*, 2020).

4. Conclusion

Adding MO at varying ratios to the CH/SPS blend

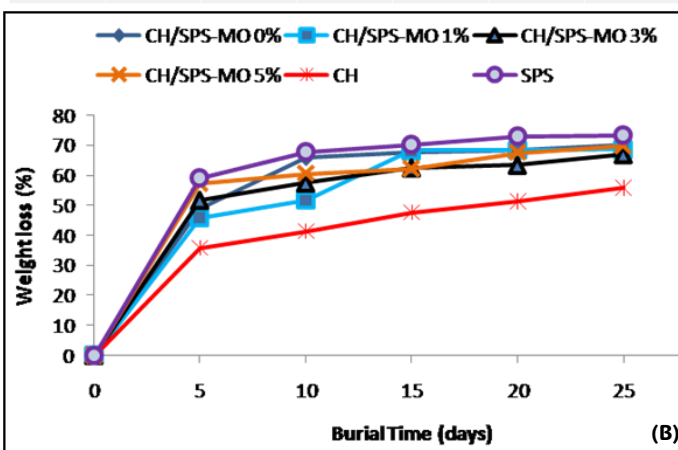
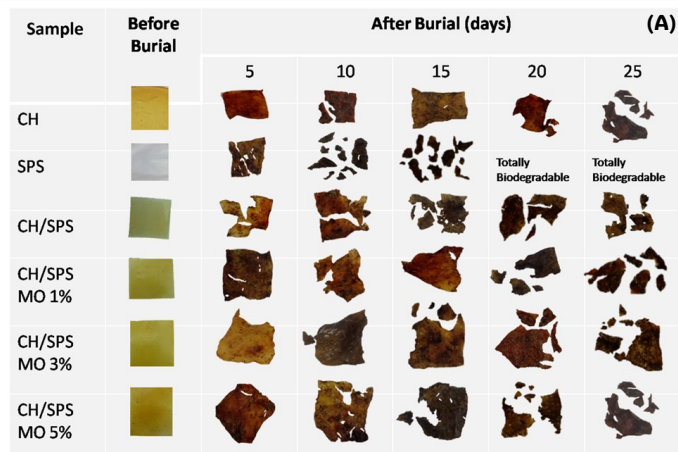


Figure 7. Soil burial: (A) physical appearance, (B) weight loss of CH/SPS-MOs films.

has been shown to optimize mechanical properties such as TS and EB, thermal stability, and antioxidant activity. The XRD results revealed that the addition of MO to the CH/SPS blend did not affect the structure of the polymeric matrix. The developed CH/SPS-MO film has satisfactory thermal stability and barrier characteristics. Based on the findings of the research, CH/SPS-MO blend films have excellent biodegradability, the potential to be used as an active film, and can substitute for the use of pure CH/SPS.

Conflict of interest

The authors declare no conflicts of interest.

Acknowledgments

The author expresses gratitude to the Ministry of Education, Culture, Research, and Technology of the Republic of Indonesia for funding the professor's research project at Universitas Syiah Kuala under the regulations outlined in Number: 65/UN11.2.1/PT.01.03/PNBP/2023.

References

- Abubakar, M.S. and Benjamin, I.A. (2019). Determination of selected engineering properties of *Moringa oleifera* seed. *Food Research*, 3(2), 96-101.

- [https://doi.org/10.26656/fr.2017.3\(2\).124](https://doi.org/10.26656/fr.2017.3(2).124)
- Arcana, I.M., Bundjali, B., Hasan, M., Hariyawati, K., Mariani, H., Anggraini, S.D. and Ardana, A. (2010). Study on properties of poly(urethane-ester) synthesized from prepolymers of ϵ -Caprolactone and 2,2-Dimethyl-1,3-Propanediol monomers and their biodegradability. *Journal of Polymers and the Environment*, 18(3), 188-195 <https://doi.org/10.1007/s10924-010-0189-9>
- Bajer, D., Janczak, K. and Bajer, K. (2020). Novel Starch/Chitosan/Aloe Vera Composites as Promising Biopackaging Materials. *Journal of Polymers and the Environment*, 28(3), 1021-1039. <https://doi.org/10.1007/s10924-020-01661-7>
- Bilbao-Sainz, C., Bras, J., Williams, T., Sénechal, T. and Orts, W. (2011). HPMC Reinforced with Different Cellulose Nano-Particles. *Carbohydrate Polymers*, 86(4), 1549-1557. <https://doi.org/10.1016/j.carbpol.2011.06.060>
- Brilhante, R.S.N., Sales, J.A., Pereira, V.S., Castelo-Branco, D.de S.C.M., Cordeiro, R.D.A., de Souza Sampaio, C.M., de Araújo Neto Paiva, M., Santos, J.B.F. dos, Sidrim, J.J.C. and Rocha, M.F.G. (2017). Research advances on the multiple uses of *Moringa oleifera*: A sustainable alternative for socially neglected population. *Asian Pacific Journal of Tropical Medicine*, 10(7), 621-630. <https://doi.org/10.1016/j.apjtm.2017.07.002>
- Caetano, K.S., Hessel, C.T., Tondo, E.C., Flores, S.H. and Cladera-Olivera, F. (2017). Application of active cassava starch films incorporated with oregano essential oil and pumpkin residue extract on ground beef. *Journal of Food Safety*, 37(4), e12355. <https://doi.org/10.1111/jfs.12355>
- Calabria, D., Mirasoli, M., Guardigli, M., Simoni, P., Zangheri, M., Severi, P., Caliceti, C. and Roda, A. (2020). Paper-based smartphone chemosensors for reflectometric on-site total polyphenols quantification in olive oil. *Sensors and Actuators: B. Chemical*, 305, 127522. <https://doi.org/10.1016/j.snb.2019.127522>
- Castillo, L.A., Farenzena, S., Pintos, E., Rodriguez, M.S., Villar, M.A., Garcia, M.A. and López, O.V. (2017). Active films based on thermoplastic corn starch and chitosan oligomer for food packaging applications. *Food Packaging and Shelf Life*, 14(Part B), 128-136. <https://doi.org/10.1016/j.fpsl.2017.10.004>
- Chinaglia, S., Tosin, M. and Degli-innocenti, F. (2018). Biodegradation rate of biodegradable plastics at molecular level. *Polymer Degradation and Stability*, 147, 237-244. <https://doi.org/10.1016/j.polymdegradstab.2017.12.011>
- Chollakup, R., Pongburoos, S., Boonsong, W., Khanonkon, N., Kongsin, K., Sothornvit, R., Sukyai, P., Sukatta, U. and Harnkarnsujarit, N. (2020). Antioxidant and antibacterial activities of cassava starch and whey protein blend films containing rambutan peel extract and cinnamon oil for active packaging. *LWT*, 130, 109573. <https://doi.org/10.1016/j.lwt.2020.109573>
- Choo, K.W., Lin, M. and Mustapha, A. (2021). Chitosan/ acetylated starch composite films incorporated with essential oils: Physicochemical and antimicrobial properties. *Food Bioscience*, 43, 101287. <https://doi.org/10.1016/j.fbio.2021.101287>
- Dai, L., Zhang, J. and Cheng, F. (2019). Effects of starches from different botanical sources and modification methods on physicochemical properties of starch-based edible films. *International Journal of Biological Macromolecules*, 132, 897-905. <https://doi.org/10.1016/j.ijbiomac.2019.03.197>
- Fang, Y., Fu, J., Tao, C., Liu, P. and Cui, B. (2019). Mechanical properties and antibacterial activities of novel starch-based composite films incorporated with salicylic acid. *International Journal of Biological Macromolecules*, 155, 1350-1358, <https://doi.org/10.1016/j.ijbiomac.2019.11.110>
- Ferreira, R.R., Souza, A.G., Nunes, L.L., Shahi, N., Rangari, V.K. and Rosa, D.D.S. (2020). Use of ball mill to prepare nanocellulose from eucalyptus biomass: Challenges and process optimization by combined method. *Materials Today Communications*, 22, 100755. <https://doi.org/10.1016/j.mtcomm.2019.100755>
- Fonseca-García, A., Jiménez-Regalado, E.J. and Aguirre-Loredo, R.Y. (2021). Preparation of a novel biodegradable packaging film based on corn starch-chitosan and poloxamers. *Carbohydrate Polymers*, 251, 117009. <https://doi.org/10.1016/j.carbpol.2020.117009>
- Frick Pavoni, J.M., Luchese, C.L. and Tessaro, I.C. (2019). Impact of acid type for chitosan dissolution on the characteristics and biodegradability of cornstarch/chitosan based films. *International Journal of Biological Macromolecules*, 138, 693-703. <https://doi.org/10.1016/j.ijbiomac.2019.07.089>
- Hasan, M., Chong, E.W.N., Jafarzadeh, S., Paridah, M.T., Gopakumar, D.A., Tajarudin, H.A., Thomas, S. and Khalil, H.P.S.A. (2019). Enhancement in the physico-mechanical functions of seaweed biopolymer film via embedding fillers for plasticulture application-A comparison with conventional biodegradable mulch film. *Polymers*, 11(2), 210. <https://doi.org/10.3390/polym11020210>
- Hasan, M., Zulfadli, Nazar, M., Rahmayani, R.F.I., Fajri,

- G. and Fansuri, H. (2019). Thermomechanical and morphology of biodegradable film made of taro starch and chitosan plasticized by castor oil. *Rasayan Journal of Chemistry*, 12(3), 1390-1398. <https://doi.org/10.31788/RJC.2019.1235326>
- Hasan, M., Rusman, R., Khaldun, I., Ardana, L., Mudatsir, M. and Fansuri, H. (2020). Active edible sugar palm starch-chitosan films carrying extra virgin olive oil: Barrier, thermo-mechanical, antioxidant, and antimicrobial properties. *International Journal of Biological Macromolecules*, 163, 766-775. <https://doi.org/10.1016/j.ijbiomac.2020.07.076>
- Hasan, M., Gopakumar, D.A., Olaiya, N.G., Zarlaida, F., Alfian, A., Aprinasari, C., Alfatah, T., Rizal, S. and Khalil, H.P.S.A. (2020). Evaluation of the thermomechanical properties and biodegradation of brown rice starch-based chitosan biodegradable composite films. *International Journal of Biological Macromolecules*, 156, 896-905. <https://doi.org/10.1016/j.ijbiomac.2020.04.039>
- Hasan, M., Khaldun, I., Zatyia, I., Rusman, R. and Nasir, M. (2022). Facile fabrication and characterization of an economical active packaging film based on corn starch-chitosan biocomposites incorporated with clove oil. *Journal of Food Measurement and Characterization*, 17, 306-316. <https://doi.org/10.1007/s11694-022-01616-7>
- Hasan, M., Rahmayani, R.F.I. and Munandar (2018). Bioplastic from Chitosan and Yellow Pumpkin Starch with Castor Oil as Plasticizer. *IOP Conference Series: Material Science and Engineering*, 333, 012087. <https://doi.org/10.1088/1757-899X/333/1/012087>
- Ilyas, R.A., Sapuan, S.M., Ibrahim, R., Abral, H., Ishak, M.R., Zainuddin, E.S., Atikah, M.S.N., Mohd Nurazzi, N., Atiqah, A., Ansari, M.N.M., Syafri, E., Asrofi, M., Herlina Sari, N. and Jumaidin, R. (2019). Effect of sugar palm nanofibrillated cellulose concentrations on morphological, mechanical and physical properties of biodegradable films based on agro-waste sugar palm (*Arenga pinnata* Wurm. Merr) starch. *Journal of Materials Research and Technology*, 8(5), 4819-4830. <https://doi.org/10.1016/j.jmrt.2019.08.028>
- Istiqomah, A., Utami, M.R., Firdaus, M., Suryanti, V. and Kusumaningsih, T. (2022). Antibacterial chitosan-Dioscorea alata starch film enriched with essential oils optimally prepared by following response surface methodology. *Food Bioscience*, 46, 101603. <https://doi.org/10.1016/j.fbio.2022.101603>
- Javaid, M.A., Zia, K.M., Zafar, K., Khosa, M.K., Akram, N., Ajmal, M., Imran, M. and Iqbal, M.N. (2020). Synthesis and molecular characterization of chitosan/starch blends based polyurethanes. *International Journal of Biological Macromolecules*, 146, 243-252. <https://doi.org/10.1016/j.ijbiomac.2019.12.234>
- Jiang, T., Duan, Q., Zhu, J., Liu, H. and Yu, L. (2020). Starch-based biodegradable materials: Challenges and opportunities. *Advanced Industrial and Engineering Polymer Research*, 3(1), 8-18. <https://doi.org/10.1016/j.aiepr.2019.11.003>
- Ju, A., Baek, S.K., Kim, S. and Song, K.B. (2019). Development of an antioxidative packaging film based on khorasan wheat starch containing moringa leaf extract. *Food Science and Biotechnology*, 28(4), 1057-1063. <https://doi.org/10.1007/s10068-018-00546-9>
- Jumaidin, R., Sapuan, S.M., Jawaaid, M., Ishak, M.R. and Sahari, J. (2016). Characteristics of thermoplastic sugar palm Starch/Agar blend: Thermal, tensile, and physical properties. *International Journal of Biological Macromolecules*, 89, 575-581. <https://doi.org/10.1016/j.ijbiomac.2016.05.028>
- Kanatt, S.R. (2020). Development of active/intelligent food packaging film containing Amaranthus leaf extract for shelf life extension of chicken/fish during chilled storage. *Food Packaging and Shelf Life*, 24, 100506. <https://doi.org/10.1016/j.fpsl.2020.100506>
- Karimi Sani, I., Pirsaa, S. and Tagi, Ş. (2019). Preparation of chitosan/zinc oxide/*Melissa officinalis* essential oil nano-composite film and evaluation of physical, mechanical and antimicrobial properties by response surface method. *Polymer Testing*, 79, 106004. <https://doi.org/10.1016/j.polymertesting.2019.106004>
- Khalil, H.P.S.A., Yap, S.W., Owolabi, F.A.T., Haafiz, M.K.M., Fazita, M.R., Gopakumar, D.A., Hasan, M. and Rizal, S. (2019). Techno-functional properties of edible packaging films at different polysaccharide blends. *Journal of Physical Science*, 30(Supp. 1), 23-41. <https://doi.org/10.21315/jps2019.30.s1.2>
- Lauriano Souza, V.G., Rodrigues, C., Ferreira, L., Alfonso Pires, J.R., Duarte, M.P., Coelho, I. and Fernando, A.L. (2019). In vitro bioactivity of novel chitosan bionanocomposites incorporated with different essential oils. *Industrial Crops and Products*, 140, 111563. <https://doi.org/10.1016/j.indcrop.2019.111563>
- Lee, K.Y., Yang, H.J. and Song, K.B. (2016). Application of a puffer fish skin gelatin film containing Moringa oleifera Lam. leaf extract to the packaging of Gouda cheese. *Journal of Food Science and Technology*, 53(11), 3876-3883. <https://doi.org/10.1007/s13197-016-2367-9>

- Luchese, C.L., Pavoni, J.M.F., dos Santos, N.Z., Quines, L.K., Pollo, L.D., Spada, J.C. and Tessaro, I.C. (2018). Effect of chitosan addition on the properties of films prepared with corn and cassava starches. *Journal of Food Science and Technology*, 55(8), 2963-2973. <https://doi.org/10.1007/s13197-018-3214-y>
- Ma, Y., Zhao, H., Ma, Q., Cheng, D., Zhang, Y., Wang, W., Wang, J. and Sun, J. (2022). Development of chitosan/potato peel polyphenols nanoparticles driven extended-release antioxidant films based on potato starch. *Food Packaging and Shelf Life*, 31, 100793. <https://doi.org/10.1016/j.fpsl.2021.100793>
- Merino, D., Mansilla, A.Y., Gutiérrez, T.J., Casalengué, C.A. and Alvarez, V.A. (2018). Chitosan coated-phosphorylated starch films: Water interaction, transparency and antibacterial properties. *Reactive and Functional Polymers*, 131, 445-453. <https://doi.org/10.1016/j.reactfunctpolym.2018.08.012>
- Moeini, A., Mallardo, S., Cimmino, A., Dal Poggetto, G., Masi, M., Di Biase, M., van Reenen, A., Lavermicocca, P., Valerio, F., Evidente, A., Malinconico, M. and Santagata, G. (2020). Thermoplastic starch and bioactive chitosan sub-microparticle biocomposites: Antifungal and chemico-physical properties of the films. *Carbohydrate Polymers*, 230, 115627. <https://doi.org/10.1016/j.carbpol.2019.115627>
- Mozafari, M.R., Flanagan, J., Matia-Merino, L., Awati, A., Omri, A., Suntres, Z.E. and Singh, H. (2006). Recent trends in the lipid-based nanoencapsulation of antioxidants and their role in foods. *Journal of the Science of Food and Agriculture*, 86(13), 2038-2045. <https://doi.org/10.1002/jsfa.2576>
- Nagar, M., Sharanagat, V.S., Kumar, Y. and Singh, L. (2020). Development and characterization of elephant foot yam starch-hydrocolloids based edible packaging film: physical, optical, thermal and barrier properties. *Journal of Food Science and Technology*, 57(4), 1331-1341. <https://doi.org/10.1007/s13197-019-04167-w>
- Nuvoli, L., Conte, P., Fadda, C., Reglero Ruiz, J.A., García, J.M., Baldino, S. and Mannu, A. (2020). Structural, thermal, and mechanical properties of gelatin-based films integrated with tara gum. *Polymer*, 214, 123244. <https://doi.org/10.1016/j.polymer.2020.123244>
- Park, J., Nam, J., Yun, H., Jin, H.J. and Kwak, H.W. (2021). Aquatic polymer-based edible films of fish gelatin crosslinked with alginate dialdehyde having enhanced physicochemical properties. *Carbohydrate Polymers*, 254, 117317. <https://doi.org/10.1016/j.carbpol.2020.117317>
- Pelissari, F.M., Andrade-Mahecha, M.M., Sobral, P.J.D.A. and Menegalli, F.C. (2017). Nanocomposites based on banana starch reinforced with cellulose nanofibers isolated from banana peels. *Journal of Colloid and Interface Science*, 505, 154-167. <https://doi.org/10.1016/j.jcis.2017.05.106>
- Riahi, Z., Priyadarshi, R., Rhim, J.W. and Bagheri, R. (2021). Gelatin-based functional films integrated with grapefruit seed extract and TiO₂ for active food packaging applications. *Food Hydrocolloids*, 112, 106314. <https://doi.org/10.1016/j.foodhyd.2020.106314>
- Riyandari, B.A. and Multazam, M. (2023). Antioxidant Profiles of Chitosan-Alginate Films with Addition of Moringa oleifera Leaf Extract for Active Packaging. *Indonesian Journal of Chemical Science*, 11(1), 1-7. <https://doi.org/10.30598/ijcr.2023.11-riy>
- Ribeiro Sanches, M.A., Camelo-Silva, C., da Silva Carvalho, C., Rafael de Mello, J., Barroso, N.G., Lopes da Silva Barros, E., Silva, P.P. and Pertuzatti, P.B. (2021). Active packaging with starch, red cabbage extract and sweet whey: Characterization and application in meat. *LWT*, 135, 110275, <https://doi.org/10.1016/j.lwt.2020.110275>
- Rodríguez, G.M., Sibaja, J.C., Espitia, P.J.P. and Otoni, C.G. (2020). Antioxidant active packaging based on papaya edible films incorporated with *Moringa oleifera* and ascorbic acid for food preservation. *Food Hydrocolloids*, 103, 105630. <https://doi.org/10.1016/j.foodhyd.2019.105630>
- Siti Waqina, A.G., Aznizam, A.B. and Sani Amril, S. (2016). Mechanical and physical properties of tapioca starch nanocomposite films. *Journal of Plastic Film and Sheeting*, 32(2), 140-162. <https://doi.org/10.1177/8756087915590189>
- Sousa, S., Costa, A., Silva, A. and Simões, R. (2019). Poly(lactic acid)/Cellulose films produced from composite spheres prepared by emulsion-solvent evaporation method. *Polymers*, 11(1), 66. <https://doi.org/10.3390/polym11010066>
- Suriyatem, R., Auras, R.A. and Rachtanapun, P. (2018). Improvement of mechanical properties and thermal stability of biodegradable rice starch-based films blended with carboxymethyl chitosan. *Industrial Crops and Products*, 122, 37-48. <https://doi.org/10.1016/j.indcrop.2018.05.047>
- Surya, I., Olaiya, N.G., Rizal, S., Zein, I., Aprilia, N.A.S., Hasan, M., Yahya, E.B., Sadasivuni, K.K. and Khalil, H.P.S.A. (2020). Plasticizer enhancement on the miscibility and thermomechanical properties of polylactic acid-chitin-starch composites. *Polymers*, 12(1), 115 <https://doi.org/10.3390/polym12010115>

- Talón, E., Trifkovic, K.T., Vargas, M., Chiralt, A. and González-Martínez, C. (2017). Release of polyphenols from starch-chitosan based films containing thyme extract. *Carbohydrate Polymers*, 175, 122-130. <https://doi.org/10.1016/j.carbpol.2017.07.067>
- Tessaro, L., Luciano, C.G., Quinta Barbosa Bittante, A.M., Lourenço, R.V., Martelli-Tosi, M. and José do Amaral Sobral, P. (2021). Gelatin and/or chitosan-based films activated with “Pitanga” (*Eugenia uniflora* L.) leaf hydroethanolic extract encapsulated in double emulsion. *Food Hydrocolloids*, 113, 106523. <https://doi.org/10.1016/j.foodhyd.2020.106523>
- Vergara-Jimenez, M., Almatrafi, M.M. and Fernandez, M.L. (2017). Bioactive components in *Moringa oleifera* leaves protect against chronic disease. *Antioxidants*, 6(4), 91. <https://doi.org/10.3390/antiox6040091>
- Yadav, S., Mehrotra, G.K., Bhartiya, P., Singh, A. and Dutta, P.K. (2020). Preparation, physicochemical and biological evaluation of quercetin based chitosan-gelatin film for food packaging. *Carbohydrate Polymers*, 227, 115348. <https://doi.org/10.1016/j.carbpol.2019.115348>
- Zain, A.H.M., Ab Wahab, M.K. and Ismail, H. (2018). Biodegradation Behaviour of Thermoplastic Starch: The Roles of Carboxylic Acids on Cassava Starch. *Journal of Polymers and the Environment*, 26(2), 691-700. <https://doi.org/10.1007/s10924-017-0978-5>
- Zeng, J., Ren, X., Zhu, S. and Gao, Y. (2021). Fabrication and characterization of an economical active packaging film based on chitosan incorporated with pomegranate peel. *International Journal of Biological Macromolecules*, 192, 1160-1168. <https://doi.org/10.1016/j.ijbiomac.2021.10.064>